1962

An electronically controlled delay line

Visvaldis Alberts Vitols
Iowa State University

AN ELECTRONICALLY CONTROLLED DELAY LINE

by

Visvaldis Alberts Vitols

A Dissertation Submitted to the
Graduate Faculty in Partial Fulfillment of
The Requirements for the Degree of
DOCTOR OF PHILOSOPHY

Major Subject: Electrical Engineering

Approved:

Signature was redacted for privacy.

In Charge of Major Work

Signature was redacted for privacy.

Head of Major Department

Signature was redacted for privacy.

Dean of Graduate College

Iowa State University
Of Science and Technology
Ames, Iowa

1962

TABLE OF CONTENTS

I. INTRODUCTION

The purpose of this project was to investigate the feasibility of obtaining variable delay by the use of a thin-film, voltage-variable-capacitor line. Of particular interest is its suitability for use in rapidly scanning phased-array receiving antennas.

At the present time there are six basic types of delay devices in common usage: (a) transmission lines, (b) distributed constant or wirewound lines, (c) lumped constant networks, (d) ultrasonic delay lines, (e) semiconductor lines, and (f) simulated delay devices. For a more thorough discussion than presented here see "Basic Types of Delay Lines" by David L. Arenberg (1).

A transmission line can be used to achieve a delay which is equal to its length divided by the velocity of propagation which is normally close to the speed of light. These normally are the best delay devices possible where a fixed delay is necessary. They have the advantages of being relatively cheap, always available, and can be quite lossless and distortionless. The chief disadvantages are size and weight. To produce different delays, switching of different lengths of cables is normally employed. One such arrangement was developed by Enslein (2) where a crossbar switching circuit is employed. A slotted line can also be used to change the delay of a cable if the output is taken at the probe. Slotted lines are very seldom used because the attenuation and cost are both high and only small variations in delay time can be achieved.

The distributed constant lines are transmission lines in which the velocity of propagation is decreased considerably from that of light. This

can be done by using high permeability or high permittivity material to increase the inductance or capacitance. More commonly the inner or outer conductors or both are coiled to increase the inductance. This also tends to increase the interturn capacitance and destroy the high-frequency performance of these lines. The performance of these lines has been increased by Kallman (3). He placed conducting strips between the inner and outer conductors but insulated from both. This tends to increase the distributed capacitance without serious distortion. Lewis and Frazier (4) have improved these lines by using a skewed helix. The mutual and self inductances of each turn can then be adjusted separately to achieve better equalization.

Lumped constant lines are, as the name implies, constructed of lumped circuit elements. These normally have bandpass characteristics which can be made lowpass, bandpass, or highpass. To achieve a wider bandpass more sections are generally required so that the line begins to approximate a distributed line.

Ultrasonic delay lines transmit the information in the form of a sound wave instead of an electromagnetic wave. These have the advantage of long delay times in a small space, however, they have high insertion loss and narrow bandpass. Ultrasonic lines can be further subdivided into solid and liquid types. The solid lines are most generally made of glass or quartz. The fixed lines use multiple reflections inside a glass polygon to increase the total path length. These are quite costly since the surfaces must be optically polished to minimize dispersion. Brouneus and Jenkins (5) have constructed a continuously variable glass delay line. This makes use of the fact that glass becomes birefringent when stressed. Here the signal is transmitted down a long glass bar. It is read out by a beam of polar-

ized light as the sound wave passes a movable slit. A delay time of 2.66 microseconds per centimeter was obtained with an upper limit in frequency of about 30 megacycles. Variable liquid lines are very similar in design to solid lines except that the medium is either water or mercury and the transducers are submersed in the liquid. In general ultrasonic lines must use a carrier because the output is a derivative of the input. The largest bandwidth achieved is about 25 - 30 megacycles with a 1000 microsecond delay.

Magnetostrictive delay lines are actually a special case of ultrasonic delay lines where the sonic signal is generated by the magnetostriction of the line itself. The line consists of a highly magnetostrictive wire around which are the read-in and read-out coils. A current pulse in one coil produces a disturbance in the section of the wire linked by the coil and this disturbance propagates acoustically along the wire. The acoustic disturbance generates a small magnetic field which is read out as it passes the read-out coil. This output signal is a derivative of the input signal so in order to reduce distortion a carrier must be used. The ferromagnetic materials used are quite lossy at higher frequencies and so a bandwidth of only about 2 to 5 megacycles is obtainable. This device has the advantages that it is relatively inexpensive and very suitable for multiple output operation. The disadvantages are the low bandwidth and high insertion loss.

Semiconductor delay lines utilize the drift of the minority carriers. The drift velocity is very dependent upon the field and thus a voltage-variable line can be constructed. However, calculations by McCue (6) indicate that the rise time obtained would be rather poor. At room temperature under optimum conditions a delay of 10 microseconds with a 1 microsecond

rise time may be expected. At lower temperatures both times would be shorter. The advantages of these lines would include the voltage variable feature and they should be relatively inexpensive. The chief disadvantages include the poor rise time, temperature dependence, and insertion loss.

Mechanical delays record the signal on some medium and then read it out at some later time. The most common of these is the tape transport mechanism. Here a continuous loop of tape or drum has the signal recorded upon it by a recording head and read out some time later by a reading head. The delay supplied can vary from a few milliseconds on up. The frequency response depends upon the tape speed and the quality of the heads. A bandwidth of about a megacycle can be obtained. Higher bandwidths may be obtained by recording different portions of the spectrum on different tracks with the low frequencies going directly to one track and the others being beat down to the low frequencies accepted by the tape. In reading out, the reverse is done by beating the appropriate channels with appropriate frequencies. These devices also require an alternating current bias in order to linearize the response. These devices are generally used for low-frequency, long delay-time applications. The advantages consist of long delay times and faithful reproduction over a limited bandwidth. The disadvantages are cost and limited bandwidth. Another mechanical delay is the "bucket brigade". This consists of a bank of capacitors which are sequentially charged to the signal voltage and then, some time later, sequentially discharged into the output. This is a sampling mechanism and for a given bank of capacitors the bandwidth is inversely proportional to the maximum delay. Depending on the type of switching circuit used, the upper frequency limit may be quite high - into hundreds of megacycles. The main

advantage is that the delay may be controlled electrically. The disadvantages are the cost, the sampling, and the size.

For more references on delay lines see Di Toro (7).

The above described delay lines are not very suitable for tuning phased-array antennas. They have to be dismissed for one or more of three reasons: high attenuation, high cost, or insufficient delay. Mechanical line stretchers may be used but these do not supply very long changes in delay. Their total cost, which includes the drive motors, is high. Their response speed is not suitable for rapidly scanning antennas. For single frequency operation, such as radar, frequency directable antennas are used. Here fixed delays of the proper magnitude to give the required phase shift are inserted between the elements of the array. The delays are chosen such that a change in frequency changes the relative phase of the elements and thus the direction of radiation or reception. This arrangement is not suitable for use in radio telescope antennas where it is desirable to have a good resolution over a band of frequencies. It is very desirable that the variable-delay lines to be used in phased-array antennas maintain a constant characteristic impedance which is independent of the delay. Voltage controlled phase shifters have been built using voltage-variable-diode capacitors and constant inductances (8). This type of arrangement, however, changes its characteristic impedance with delay.

By using thin magnetic films as variable inductances it is possible to construct a line which maintains a constant characteristic impedance.

This line is best suited for receiving applications as it is a small-signal device. The voltage-variable capacitors are connected directly across the line and thus would give undesirable harmonics if a large volt-

age were applied across them. When used in array antennas this line is not intended to produce the total delay necessary in phasing the extremal antenna elements. Most of the delay would be obtained by switching of long delay cables. This electrically controlled delay line would be used as the vernier once the rough adjustment has been achieved by the fixed long cables. Two reasons make it desirable to use cables for the rough adjustment. The electrically variable line is lossier and also more expensive than regular cable.

Once a device of this type is made other possible uses suggest themselves. Among these are phase modulation, pulse-time modulation, phase control of high-frequency signals, and the determination of the autocorrelation or crosscorrelation function of high-frequency signals.

II. DESCRIPTION

A. General

The wave velocity in a distributed lossless transmission line is given by

$$v = \frac{1}{\sqrt{LC}} \tag{1}$$

and the delay by

$$d = \sqrt{LC} \tag{2}$$

where

L-inductance in henries per meter

C-capacitance in farads per meter

v-velocity of the wave in meters per second

and d-delay in seconds per meter

Thus it can be seen that the delay per unit physical length of the line can be changed by changing either the inductance or capacitance or both. And the resulting delay is given by equation (2).

It was stated earlier that it is also very desirable to keep the characteristic impedance constant. For a lossless line the characteristic impedance is

$$Z_o = \sqrt{\frac{L}{C}} \tag{3}$$

where

Z_o = characteristic impedance in ohms and other terms as previously defined

Thus to maintain a constant characteristic impedance the inductance to ca-

pacitance ratio must remain constant. It would be very desirable to construct a line where the inductance and the capacitance are uniformly distributed. This would call for a strip of magnetic film the length of the line and also the voltage-variable capacitor to be of the same length. If this distributed line had negligible loss, it would then satisfy the above equations and give a truly variable delay. However, with the equipment available, it would be extremely difficult to construct a distributed line. Thus for simplicity of construction the line that was constructed was a single-wire-above-ground transmission line. The wire was coated with an axially magnetized coating of permalloy, this to give the variable inductance. See Fig. 2. To obtain the variable capacitance voltage-variable-capacity diodes are inserted periodically between the wire and ground.

B. Variable Inductance

A thin permalloy film may be used to change the effective inductance of a coil. To achieve this the coil is positioned in such a way that its field acts on the film in the hard direction, i.e., the magnetic field of the coil is at right angles to the rest position of the magnetization vector of the film, as shown in Fig. 1. When some current flows in the coil it produces a field which tends to rotate the magnetization vector away from its rest position. When this is done some of the flux from the magnetization links turns of the coil. The amount of flux depends on the amount of rotation and this in turn upon the stiffness of the magnetization vector. The stiffness can be changed by a field in the easy direction. So the effective permeability seen in the hard direction depends on the field in the easy direction. To determine the above relationship consider the

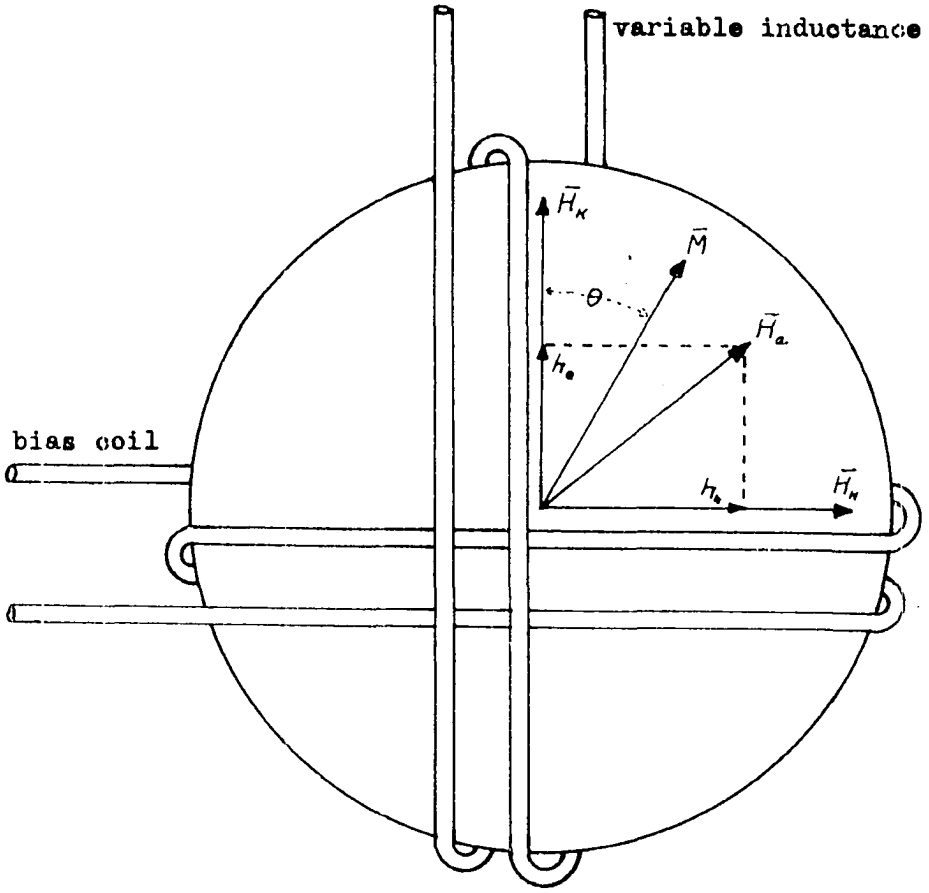

Fig. 1. Definitions of field directions

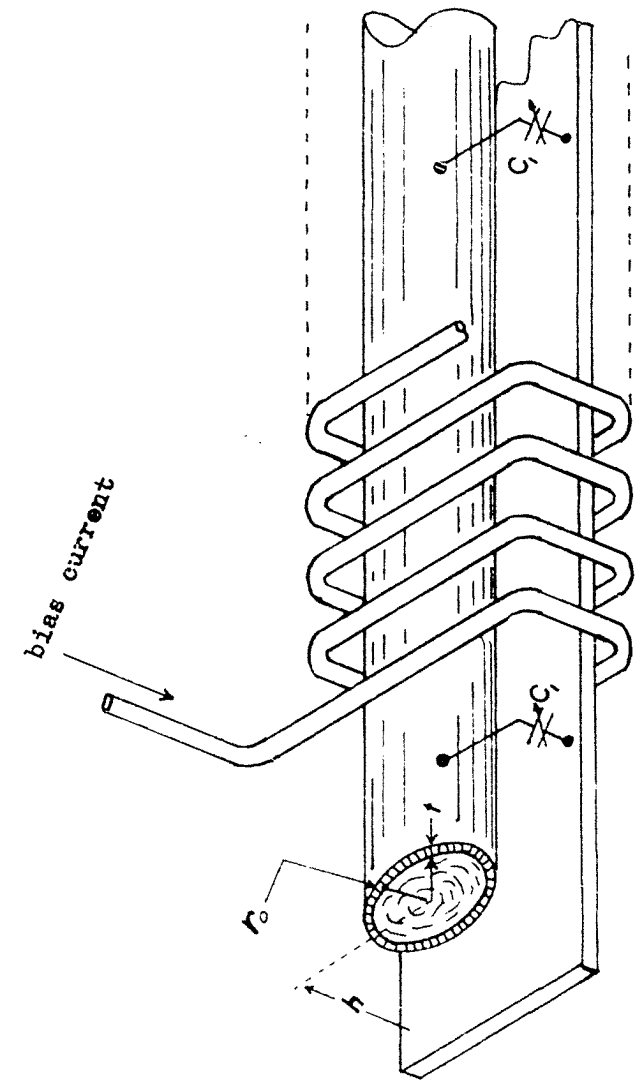

Fig. 2. Pictorial of the arrangement used

total energy of the film. The total energy is the sum of the magnetocrystalline anisotropy energy, the energy due to the applied field, the wall energy, and the shape-factor energy.

The magnetocrystalline anisotropy energy, further referred to simply as anisotropy energy, is caused by the displacement of the magnetization vector from a preferred crystal direction. This is a property of the crystalline structure alone and does not depend upon the crystal's macro-shape or any external fields. The anisotropy energy is given by

$$E_{an} = \frac{H_k M}{2} \sin^2 \theta \tag{4}$$

where

E_{an}-anisotropy energy

M -magnetization

θ -angle between M and the preferred direction (due to the crystalline structure only) of M

H_k -anisotropy field

The anisotropy field is not a true field existing in the crystal, it is an equivalent field which is used to represent the internal crystalline forces acting upon the magnetization vector. The applied field energy is

$$E_{ap} = - \overline{H}_a \cdot \overline{M} \tag{5}$$

where

E_{ap}-energy due to the applied field

H_a -applied field

As the name implies the wall energy is the energy added to the total energy by the formation of domain walls. Between two oppositely magnetized domains

the individual dipoles slowly rotate from one atom to the next going from one domain to the other. The wall energy is actually the sum of two energies, the exchange energy and the anisotropy energy. The exchange energy is due to interatomic forces which tend to align the spins, or magnetic dipoles, of neighboring atoms. This energy is inversely proportional to the wall thickness. The anisotropy energy is directly proportional to the wall thickness. Then the actual wall thickness is going to be such that the sum of the two energies is a minimum. In the arrangement considered here the film is considered to be a single domain and thus wall energy is not present.

The shape-factor energy is associated with the demagnetizing field and is dependent upon the shape of the sample. This field (H_d) is highest in the smallest dimension of the sample and lowest in the largest. In this case the film is very thin and thus the demagnetizing field perpendicular to the plane of the film is very high. This keeps the magnetization vector practically in the plane of the film. Since the film is round there is no preference in any direction in the plane of the film. So in this case the shape energy is constant and therefore will not be considered.

Then the total energy of interest is the sum of the anisotropy energy and the applied field energy

$$W = \frac{H_k M}{2} \sin^2\theta - \bar{H}_a \cdot \bar{M} \qquad (6)$$

where

W = the total energy of interest

and other terms as previously defined. Resolving the applied field (H_a) into its components

$$\bar{H}_a = \bar{e}_h h_h + \bar{e}_e h_e \tag{7}$$

then

$$W = \frac{H_k M}{2} \sin^2\theta - h_e M \cos\theta - h_h M \sin\theta \tag{8}$$

The magnetization will always assume a direction to minimize the total energy W for any applied field. To find the energy minimum the derivative of the energy with respect to the angle is set equal to zero

$$\frac{\partial W}{\partial \theta} = \frac{H_k M}{2} 2 \sin\theta \cos\theta + h_e M \sin\theta - h_h M \cos\theta = 0 \tag{9}$$

By rearranging terms

$$\sin\theta = \frac{h_h}{H_k + h_e \cos\theta} \tag{10}$$

If h_h is small compared to H_k, then θ is small and $\cos\theta \approx 1$.

Then

$$\sin\theta \approx \frac{h_h}{H_k + h_e} \tag{11}$$

Now

$$B_h = M \sin\theta \tag{12}$$

and substituting (11) into (12)

$$B_h \approx M \frac{h_h}{H_k + h_e} \tag{13}$$

and

$$\mu_h = \frac{B_h}{h_h} \approx \frac{M}{H_k + h_e} \tag{14}$$

where

B_h = flux density in the hard direction

μ_h = effective permeability in the hard direction

This equation holds for h_h small compared to H_k. The physical arrangement shown in Fig. 1 does not give a very large percentage of inductance change. Since the films are deposited on a glass substrate and the glass has a much greater cross-sectional area than the film the total flux through the glass is large compared to the film flux. So even though there is a large change in the relative permeability of the film this can not be exploited by the above arrangement.

In order to increase the flux linkage and decrease the stray flux the arrangement shown in Fig. 2 was used as the variable inductance. A small copper wire was coated with a thin permalloy film* with its easy direction parallel to the length of the wire and the hard direction circumferential to the wire. The specific wire used was 5 mils in diameter with a 15 micron permalloy film. Equation (14) can still be used in calculating the inductance of the wire. In this case there is no demagnetizing field present because there are no edges to the film. In the previous case the demagnetizing field was constant and therefore did not contribute to any changes in energy; here the demagnetizing field is again constant (zero) and also does not contribute to any changes in energy. The film is also in a single domain and so there is no wall energy just as before. The bias field tends to prevent the breaking of the film into multiple domains. The

---

*The permalloy coated wire was donated by F. N. Long of Bell Telephone Laboratories.

remaining three energies: anisotropy, wall, and shape would all be increased by the breakup of the single domain.

The inductance will be calculated for two cases: 1) for low frequencies; 2) for high frequencies near cutoff. For low frequencies the current may be considered to be uniformly distributed in the copper wire since the permalloy has about ten times the resistivity and about one fortieth the cross-sectional area of the copper. The total flux linkage consists of three parts: 1) internal, 2) permalloy, and 3) external. The flux density inside a current carrying conductor for a uniform current distribution is

$$B = \frac{\mu_o \mu_r I(r^2)}{2\pi r\ (r_o^2)} \tag{15}$$

The differential flux linkage is

$$d\lambda_1 = \frac{\mu_o \mu_{r1}\ I\ r^3\ dr}{2\pi\ r_o^4} \tag{16}$$

and the internal flux linkage is then

$$\lambda_1 = 5 \times 10^{-8} \mu_{r1}\ I \tag{17}$$

where

μ_1 -internal flux linkage of the conductor

μ_{r1}-relative permeability of the conductor

I -total current

r_o -radius of the wire

Since all of the current is considered to flow in the copper, the field that is seen by the permalloy is

$$H_h = \frac{I}{2\pi r_o} \tag{18}$$

Then

$$B_h = \frac{\mu_h I}{2\pi r_o} \tag{19}$$

and

$$\phi_p = \frac{\mu_h I t}{2\pi r_o} \tag{20}$$

Therefore, the flux linkage due to permalloy is

$$\lambda_p = \frac{\mu_h I t}{2\pi r_o} \tag{21}$$

where

t = thickness of the permalloy

λ_p = flux linkage due to permalloy

The external flux linkage between two cylindrical conductors is

$$\lambda = 4 \times 10^{-7} I \mu_r \ln \frac{2h}{r_o} \tag{22}$$

where

$2h$ = the spacing between the conductors

For the case of a single wire above a ground plane there will be half the flux for the same current so the linkage there is

$$\lambda_2 = 2 \times 10^{-7} I \mu_{r2} \ln \frac{2h}{r_o} \tag{23}$$

where

λ_2 = external flux linkage

μ_{r2} = relative permeability of the dielectric material

h = spacing between the ground plane and the center of the wire

Then the total flux linkage is

$$\lambda_t = \lambda_1 + \lambda_p + \lambda_2 \tag{24}$$

$$= 2 \times 10^{-7} I \left(\mu_{r1} 0.25 + \mu_n \frac{t}{r_o} + \mu_2 \ln \frac{2h}{r_o} \right) \tag{25}$$

Substituting in for the permeabilities and dividing through by the current, the total inductance is

$$L_{lf} = 2 \times 10^{-7} \left(0.25 + \frac{Mt}{\mu_o (h_k + h_e) r_o} + \ln \frac{2h}{r_o} \right) \tag{26}$$

where

L_{lf} = the total low frequency inductance

The above inductance equation is valid when the frequency is low enough such that the current may be considered to be uniformly distributed throughout the wire.

In the high-frequency case the current will be crowded near the surface of the conductor. The case that is considered here is the one where the frequency is high enough so that all of the current may be considered to be flowing in the permalloy coating. At first glance it may appear that an exceedingly high frequency is required to make the depth of penetration less than the 1.5 micron thickness of the permalloy film. This, however, is not the case because of the extremely high permeability of the permalloy. So the inductance will be developed with the above assumptions. The total high-frequency inductance consists of the internal inductance term plus the external inductance term. To calculate the internal inductance of the wire consider the internal impedance of an infinitely long strip $2\pi r_o$ meters wide.

$$Z_{hf} = \frac{R_s(1+j)}{2\pi r_o} \tag{27}$$

then

$$R_{hf} = (L_i)_{hf} = \frac{R_s}{2\pi r_o} = \frac{1}{r_o}\sqrt{\frac{f\mu}{4\sigma\pi}} \tag{28}$$

and

$$L_i = \frac{1}{4 r_o \pi^{3/2}}\sqrt{\frac{\mu}{\sigma f}} \tag{29}$$

where

L_i = internal inductance

σ = conductivity of permalloy

f = frequency of operation

The external inductance is the same as before. Thus the total high-frequency inductance is

$$L_{hf} = \frac{1}{4\pi r_o}\left[\frac{M}{(H_k + h_e)(\sigma f \pi)}\right]^{1/2} + \frac{\mu_o}{2\pi}\ln\frac{2h}{r_o} \tag{30}$$

C. Capacitance

The total capacitance of the line is the sum of the constant-distributed capacitance and the variable-diode capacitance. The distributed capacity is

$$C_d = \frac{2\pi\epsilon_o K}{\ln\left[\frac{h}{r_o} + \sqrt{\left(\frac{h}{r_o}\right)^2 - 1}\right]} \tag{31}$$

where

C_d = distributed capacity in farads per meter

ϵ_o = permitivity of free space

K = dielectric constant of the dielectric

The capacitance of the voltage-variable capacitors is plotted as a function of bias voltage in Fig. 3. Of the diodes tested most had their capacitance within 5% of the values shown in Fig. 3, and only one deviated by 15%. So the curve can be assumed to be a fairly accurate representation of the capacitance.

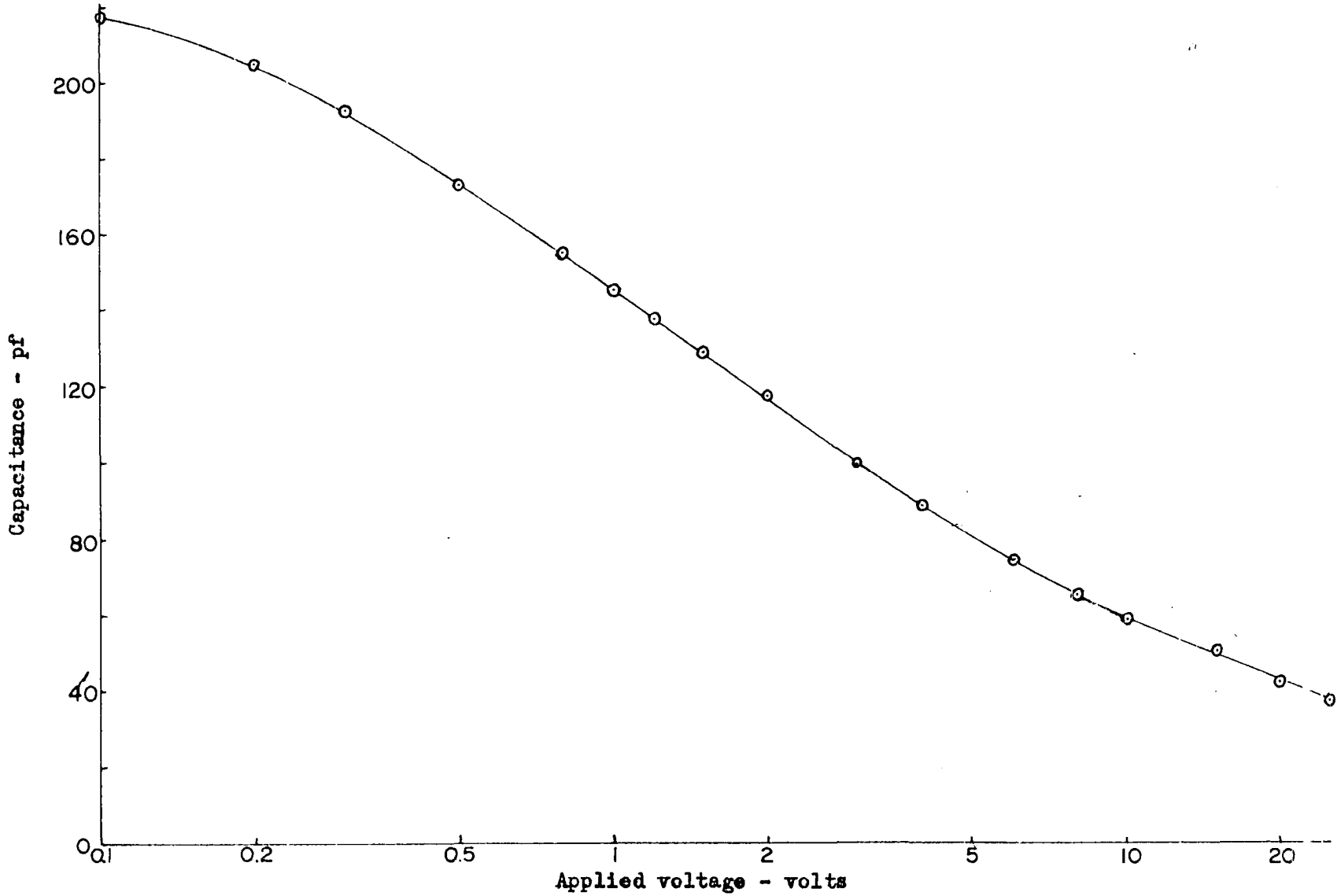

Fig. 3. Diode capacitance v. s. applied voltage

III. TRANSMISSION CHARACTERISTICS

If the variable capacitance as well as the inductance were uniformly distributed, the line would act as an ideal transmission line of variable length - within physical limitations. However, since due to physical reasons it is necessary to have lumped capacitors the transmission characteristics change drastically at high frequencies. The purpose of this section is to determine the frequency dependence of the lumped line. The first calculation will be the propagation constant of a loaded line. The term "loaded line" as used here refers to a transmission line with periodic capacitances and does not refer to the termination of the line.

Consider the periodically loaded line in Fig. 4. Arbitrarily cut the line into sections l_a and l_b such that: $l = l_a + l_b$ where l is the spacing of the capacitors. Also let the capacitors be contained in the l_a's. Now the line is considered to be made up of short sections of lines with two different characteristics. Each l_b section has L henries per meter of inductance and C farads per meter of capacitance. Each l_a section has also L henries of inductance but C_1/l_a farads per meter of capacitance. Here C_1 is the capacitance of each capacitor. Actually the capacitance per meter in each l_a section is $C + C_1/l_a$ but when the limit as $l_a \longrightarrow 0$ is taken C becomes negligible compared to C_1/l_a. So for convenience it will be dropped out now. The time independent wave equation

$$\frac{\partial^2 V}{\partial x^2} - k^2 V = 0 \tag{32}$$

has to be satisfied for each section. In section "a" $k = k_a$ and section "b" $k = k_b$. Then for the whole line

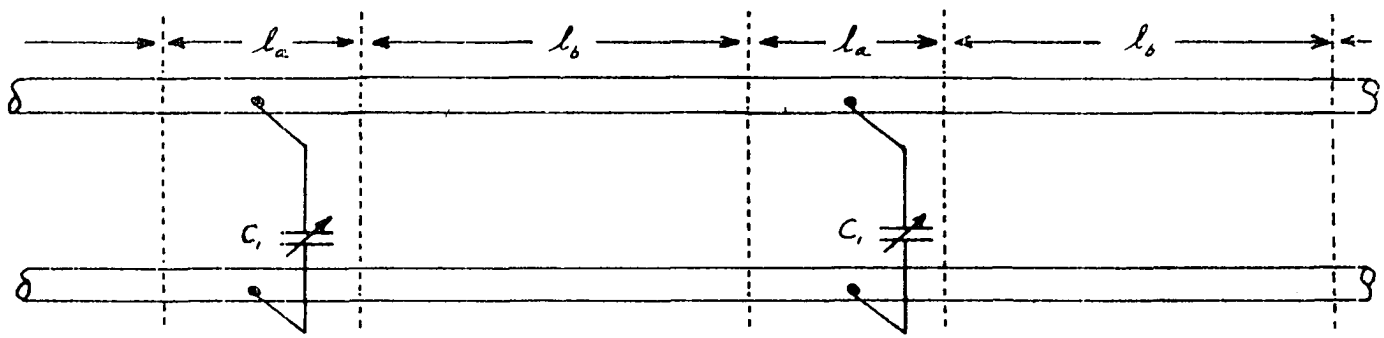

Fig. 4. Definitions of line parameters

$$\frac{\partial^2 V}{\partial x^2} + \lambda(x)\, V = 0 \tag{33}$$

must be satisfied where

$$\lambda(x) = -k_a^2 \quad \text{for} \quad -l_a < x < 0$$
$$\lambda(x) = -k_b^2 \quad \text{for} \quad 0 < x < l_b$$

This has the form of Hill's equation. The solutions in each section separately are

$$V(x) = A \exp(k_a x) + B \exp(-k_a x) \quad \text{for} \quad -l_a < x < 0 \tag{34}$$
$$V(x) = C \exp(k_b x) + D \exp(-k_b x) \quad \text{for} \quad 0 < x < l_b \tag{35}$$

Now by Floquet's theorem (see pp. 381-384 of Ince (9))

$$V(x) = E(x) \exp(\mu x) \tag{36}$$

where $E(x)$ is periodic in x with period 1

Then

$$V(x) = V(x - l_a - l_b) \exp[\mu(l_a + l_b)] \tag{37}$$

Now substituting (34) into (37)

$$V(x) = A \exp[\mu(l_a + l_b)] \exp[k_a(x - l_a - l_b)]$$
$$+ B \exp[\mu(l_a + l_b)] \exp[k_a(-x + l_a + l_b)] \tag{38}$$

The function must be continuous at $x = 0$ and $x = l_b$ to make the voltage continuous and the first derivative must be continuous to make the current continuous. To satisfy the boundary conditions at $x = 0$

$$A + B = C + D \tag{39}$$

illegible (40)

and at $x = l_b$

$$A \exp[\mu (l_a + l_b) - k_a l_a] + B \exp[\mu(l_a + l_b + k_a l_a] = C \exp[k_b l_b] + D \exp[- k_b l_b] \quad (41)$$

$$Ak_a \exp[\mu (l_a + l_b) - k_a l_a] - Bk_a \exp[\mu(l_a + l_b) + k_a l_a] = Ck_b \exp[k_b l_b] - Dk_b \exp[- k_b l_b] \quad (42)$$

The above four equations in A, B, C, and D will have a solution only if their determinant is equal to zero. Setting the determinant equal to zero, expanding, and rearranging terms gives

$$\exp[2\mu(l_a + l_b)] - 2 \exp[\mu(l_a + l_b)] \left\{ \cosh k_a l_a \cosh k_b l_b + \frac{1}{2}\left[\frac{k_a}{k_b} + \frac{k_b}{k_a}\right] \sinh k_a k_a \sinh k_b l_b \right\} + 1 = 0 \quad (43)$$

Combining the exponential terms and rearranging gives

$$\cosh[\mu(l_a + l_b)] = \cosh k_a l_a \cosh k_b l_b + \frac{1}{2}\left[\frac{k_a}{k_b} + \frac{k_b}{k_a}\right] \sinh k_a l_a \sinh k_b l_b = 0 \quad (44)$$

Let

$$\beta_1^2 = - k_a^2 \text{ and } \beta_2^2 = - k_b^2$$

Then

$$\beta_1^2 = \omega^2 L \frac{C_1}{l_a} = - k_a^2 \quad \text{and} \quad k_a = j\omega \sqrt{\frac{LC_1}{l_a}} \quad (45)$$

$$\beta_2^2 = \omega^2 LC = - k_b^2 \quad \text{and} \quad k_b = j\omega \sqrt{LC} \quad (46)$$

Next, substituting (45) and (46) into (44) leads to

$$\cosh[\mu(l_a + l_b)] = \cosh j\omega\sqrt{LC_1}l_a \cosh j\omega l_b\sqrt{LC}$$
$$+ \frac{1}{2}\left[\sqrt{\frac{C_1}{l_a C}} + \sqrt{\frac{C l_a}{C_1}}\right] \sinh j\omega\sqrt{LC_1}l_a \sinh j\omega l_b\sqrt{LC} \quad (47)$$

Now the limit is taken as $l_a \to 0$ and $l_b \to l - l_a$. The first term and the second part of the second term on the right hand side present no problems. The term

$$\lim_{l_a \to 0} \sqrt{\frac{C_1}{l_a C}} \sinh j\omega\sqrt{LC_1}l_a \sinh j\omega l_b\sqrt{LC} \quad (48)$$

becomes undefined. Rewriting and taking the limit gives

$$\lim_{l_a \to 0}\left\{\frac{\sin\omega\sqrt{LC_1}l_a}{\omega\sqrt{LC_1}l_a}\right\} j\omega C_1\sqrt{\frac{L}{C}} \sinh j\omega l_b\sqrt{LC}$$

$$= j\omega C_1\sqrt{\frac{L}{C}} \sinh j\omega l_b\sqrt{LC} \quad (49)$$

and the limit of equation (47) is

$$\cosh\mu l_b = \cosh(j\omega\sqrt{LC}\, l_b) + \frac{j\omega C_1}{2}\sqrt{\frac{L}{C}} \sinh(j\omega\sqrt{LC}\, l_b) \quad (50)$$

By letting

$$\mu = j\gamma$$

$$\beta_2 = \beta$$

$$l_b = l \quad (\text{since } l \to l_b \text{ and } l_a \to 0)$$

and making the substitutions and converting to trigonometric form, equation (50) becomes

$$\cos \gamma l = \cos \beta l - \beta l \left(\frac{l}{2}\right) \frac{C_1}{lC} \sin \beta l \qquad (51)$$

where γ is the propagation constant for the loaded line. Propagation takes place when γ is real and attenuation when it is imaginary. This equation, (51), has a real γ as its solution only for certain ranges of β. The propagation constant γ is plotted as a function of β with $\frac{C_1}{lC}$ as a parameter in Fig. 5. The free-line propagation constant β is directly proportional to frequency. The graph is shown for $0 \leq \gamma \leq 2\pi$, for larger values the gaps become wider and the line sections more vertical. In the limit they are straight line segments connecting the point $\beta = n\pi$, $\gamma = n\pi$ with $\beta = n\pi$, $\gamma = (n + 1)\pi$. This means that the pass bands become narrower until they are discrete frequencies such that $\frac{n\lambda}{2} = l$, where λ is the wavelength in an unloaded line. There will be no distortion if all of the frequency components are in the straight line portion of the first passband. Thus it can be seen from Fig. 5 that for wider passband the loading of the line must be slight.

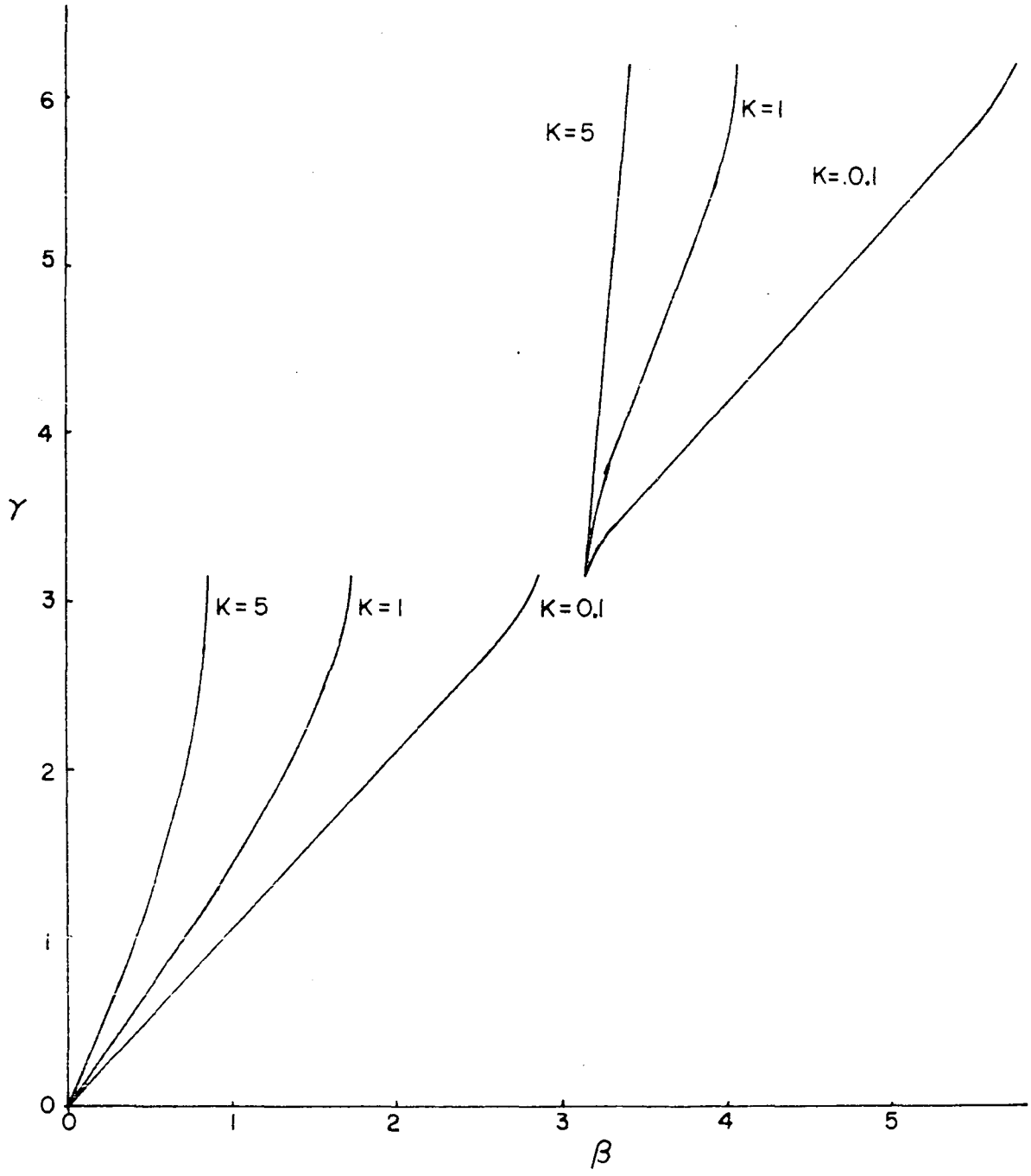

Fig. 5. Propagation constant for a loaded line

IV. CHARACTERISTIC IMPEDANCE

In order to maintain a constant characteristic impedance the inductance to capacitance ratio must be kept constant. This maintains the impedance constant when the spacing between the variable capacitors is small compared to a wavelength. When the capacitor spacing becomes an appreciable part of a wavelength the characteristic impedance is no longer the same as for low frequencies. In this section the impedance as a function of frequency (or more specifically as a function of β) will be determined. In this case an infinitely long line will be considered to consist of sections each 1 meters long (1 is the spacing of the capacitors) with the capacitors located in the center of each section. Fig. 6 shows the n th section of the line. This section sees some impedance, say Z_L, at its right-hand terminals. Now if the characteristic impedance of the line without the capacitors is Z_o then the impedance just to the right of the capacitor, point "a" in Fig. 6, looking toward the right is

$$Z_a = Z_o \frac{Z_L \cosh \gamma \frac{l}{2} + Z_o \sinh \gamma \frac{l}{2}}{Z_o \cosh \gamma \frac{l}{2} + Z_L \sinh \gamma \frac{l}{2}} \tag{52}$$

where

Z_a = impedance at point "a" looking toward Z_L

Z_L = impedance seen by the n th section looking toward the (n + 1) st section

Z_o = characteristic impedance of the line without the capacitances

l = distance between the capacitors

γ = propagation constant for the line when all C_1's are zero (53)

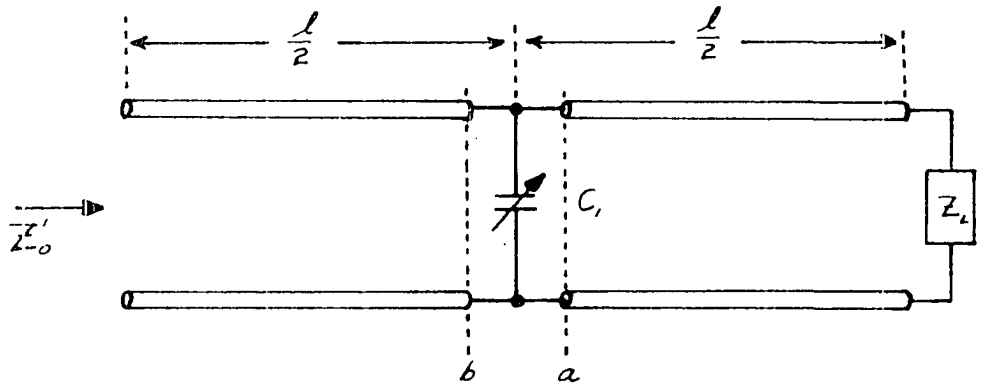

Fig. 6. Definitions of line parameters for impedance calculations

The impedance at point "b" looking toward the right is

$$Z_b = \frac{Z_a}{1 + j\omega C_1 Z_a} \tag{54}$$

And Z_L' (the impedance looking into the n th section) is

$$Z_L' = Z_o \frac{Z_b \cosh \gamma \frac{1}{2} + Z_o \sinh \gamma \frac{1}{2}}{Z_o \cosh \gamma \frac{1}{2} + Z_b \sinh \gamma \frac{1}{2}} \tag{55}$$

Since characteristic impedance is defined as the impedance which appears at the input terminals when the same impedance is placed across the output terminals, then $Z_L' = Z_L = Z_o'$ = characteristic impedance of the loaded line. Now substituting Z_o' for Z_L and Z_L' and solving for Z_o' leads to

$$Z_o' = Z_o \left[\frac{\sinh \gamma l + j \frac{\omega C_1 Z_o}{2} (\cosh \gamma l - 1)}{\sinh \gamma l + j \frac{\omega C_1 Z_o}{2} (\cosh \gamma l + 1)} \right]^{1/2} \tag{56}$$

The only restriction on this equation is that C_1 is lossless. For the case where the line is lossless the equation may be simplified to

$$Z_o' = Z_o \left[\frac{\sin \beta l + \frac{K}{2} \beta l (\cos \beta l - 1)}{\sin \beta l + \frac{K}{2} \beta l (\cos \beta l + 1)} \right]^{1/2} \tag{57}$$

where

$$K = \frac{C_1}{lC}$$

$$\beta = \omega \sqrt{LC}$$

For low frequencies ($\beta \to 0$), equation (57) reduces to

$$Z_{1f} = Z_o' \Big|_{\beta \to o} = \frac{Z_o}{\sqrt{1 + K}} \tag{58}$$

Fig. 7 gives the first passband of $\frac{Z_o'}{Z_{1f}}$ as a function of β 1 with K as a parameter. There are more passbands for higher values of β 1. However, these are narrower and their impedance characteristics are not smooth. Only the first band is of interest here. For low values of K the impedance is quite constant over most of the passband and then goes rapidly to zero near the cutoff. For higher values of K the impedance starts to droop much faster and also reaches zero much sooner.

From equation (57) it can be obtained that the characteristic impedance will be zero when

$$K \frac{\beta 1}{2} \tan \frac{\beta 1}{2} = 1 \tag{59}$$

The solution of this trancedental equation for β 1 is plotted in Fig. 8 as a function of K. For a given K the line propagates if β 1 is less that the solution of equation (59) and attenuates when it is greater.

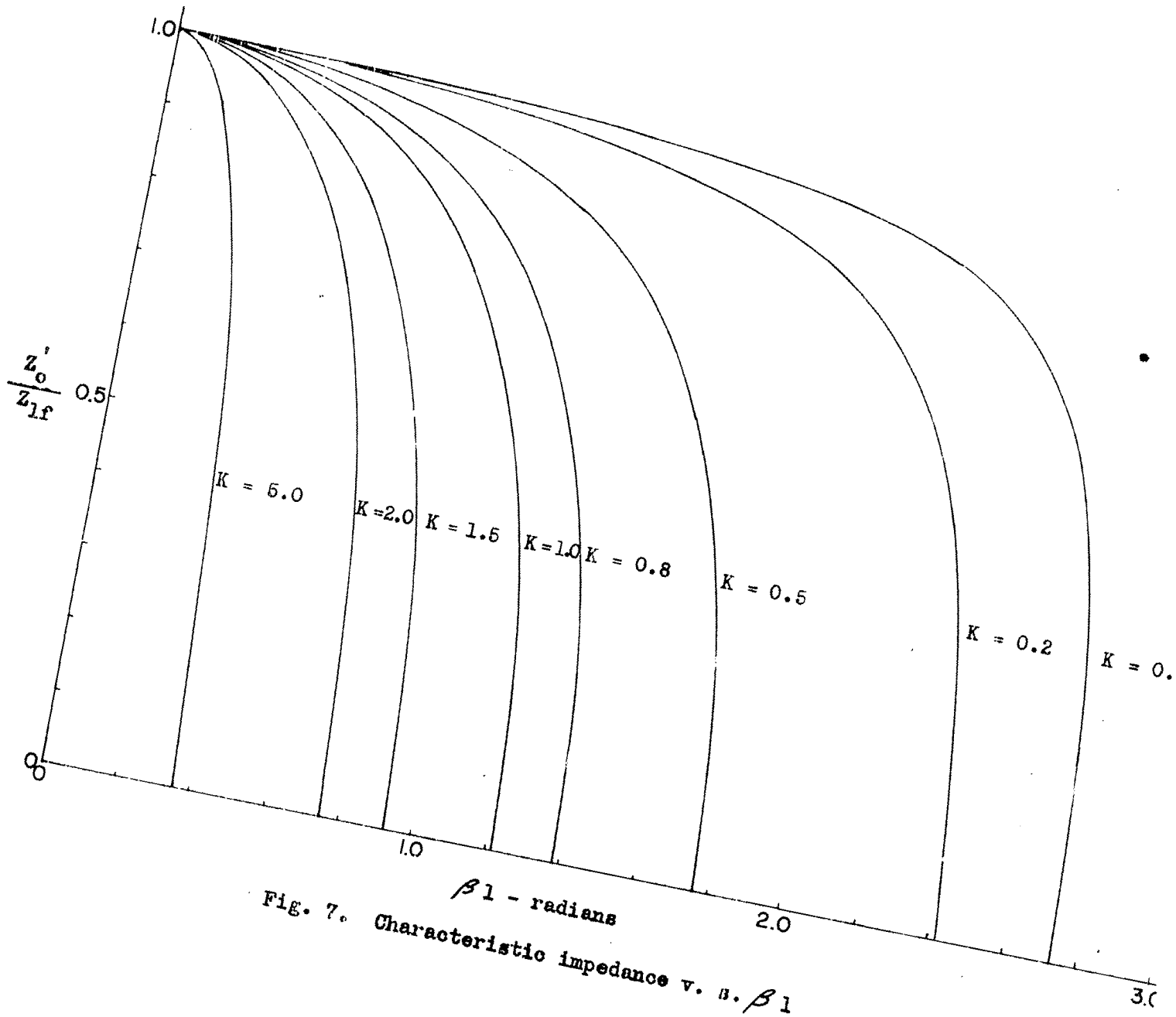

Fig. 7. Characteristic impedance v. s. β_1

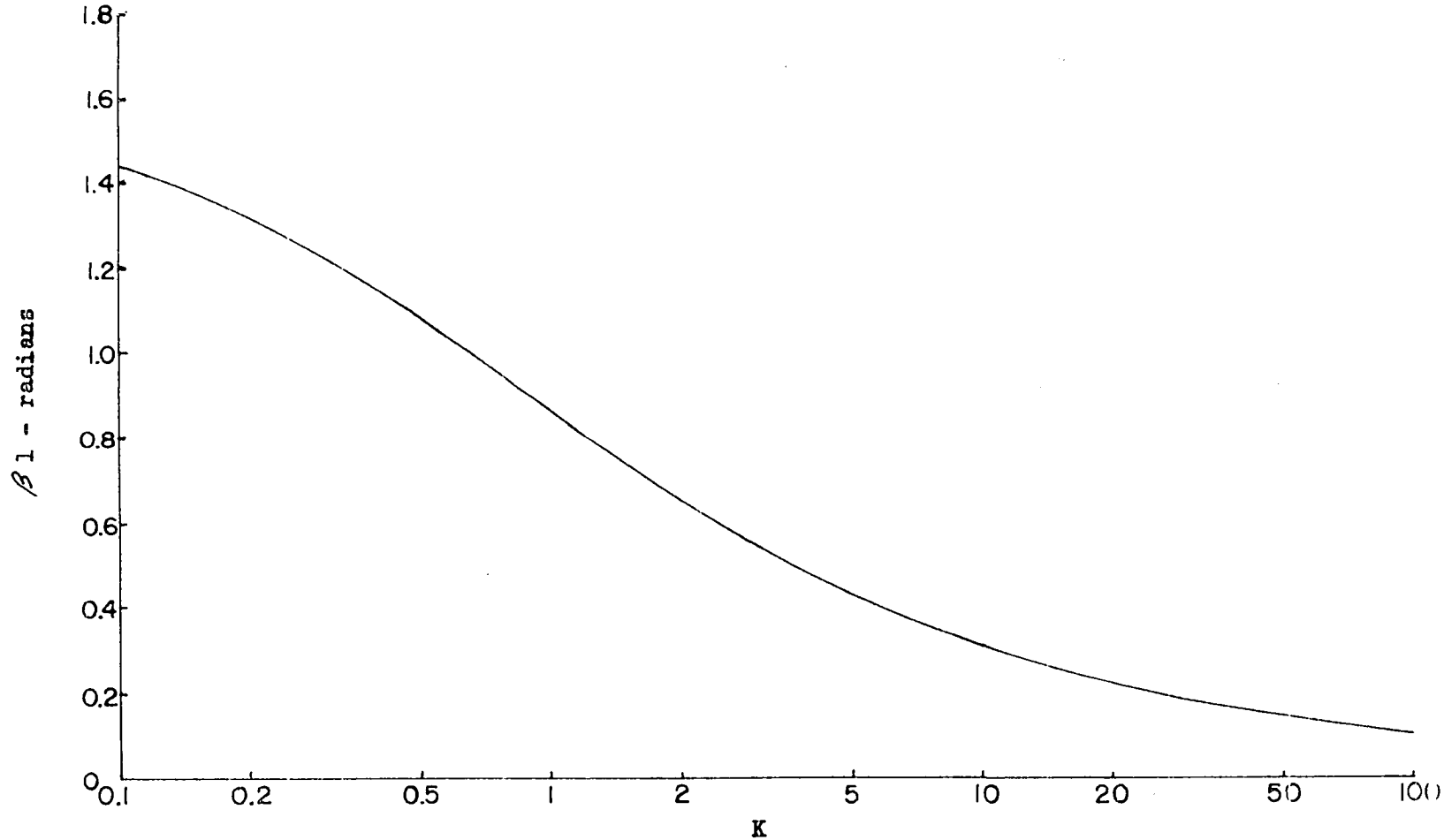

Fig. 8. Cut off phase shift v. s. loading

V. DELAY OF THE LINE

For a uniformly distributed lossless line the delay is simply $\sqrt{LC}$. Here, however, the line is neither distributed nor lossless. So the delay will have a more complicated expression. A second problem also arises--i.e., in general the output does not have the same shape or amplitude as the input. Where this is the case it becomes difficult to define any one thing as the delay. There are three possible definitions of delay that are used for different purposes: "delay," "phase delay," and "group delay". They are defined as follows:

$$\text{"delay"} = \left.\frac{d\theta}{d\omega}\right|_{\omega = 0} \tag{60}$$

$$\text{"phase delay"} = \left.\frac{\theta}{\omega}\right|_{\omega = \omega_0} \tag{61}$$

$$\text{"group delay"} = \left.\frac{d\theta}{d\omega}\right|_{\omega = \omega_0} \tag{62}$$

where

θ = phase angle

ω = angular velocity

"Delay" is the derivative of the phase angle with respect to angular velocity evaluated at zero angular velocity. If the derivative is the same from zero angular velocity to some θ then for signals with no components of angular velocity higher than ω_0 the device acts as a distortionless delay device. "Phase delay" is the quotient of the phase angle and the operating frequency. It may be thought of as a given delay only for that one frequency, a different frequency may have a different delay. Therefore, a

nonsinusoidal signal will undergo distortion in passing through this type of device. "Group delay" is the derivative of the phase angle with respect to the angular velocity evaluated at ω_o. The same applies to group delay as to delay with the frequency band now centered around ω_o. This is mainly of interest in cases where a carrier is modulated to produce some side bands and the effect of the device upon the signal is of interest. If the slope of the $\theta - \omega$ curve is constant throughout the bandwidth of the signal then no distortion will take place. The main interest here is in "delay". The "delay" of the line was calculated from the total inductance and capacitance per unit length. The high-frequency inductance from equation (30) was used because the experimental delay of a pulse will later be compared to these curves. The capacitance used was $C_d + \frac{C_1}{I}$. The calculated "delay" is shown as curve #1 in Fig. 9. The calculated "phase delay" is in Fig. 9 as curve #2. This was calculated from the equation

$$\text{"phase delay"} = \frac{\operatorname{Im} \gamma}{\omega} \tag{63}$$

The two curves are seen to be separate for large delays and to converge for small delays. Some of this is due to scaling (i.e., constant ratio of impedance to resistance) but most of it is caused by the high bias field on the permalloy. The increased bias decreases the permeability and this in turn increases the depth of penetration. When the depth of penetration is about the thickness of the permalloy, or greater, more and more of the current starts to flow in the copper. This causes an increase in the inductance-to-resistance ratio. In other words, when the resistance and inductance approach the low-frequency case the above formula is no longer valid.

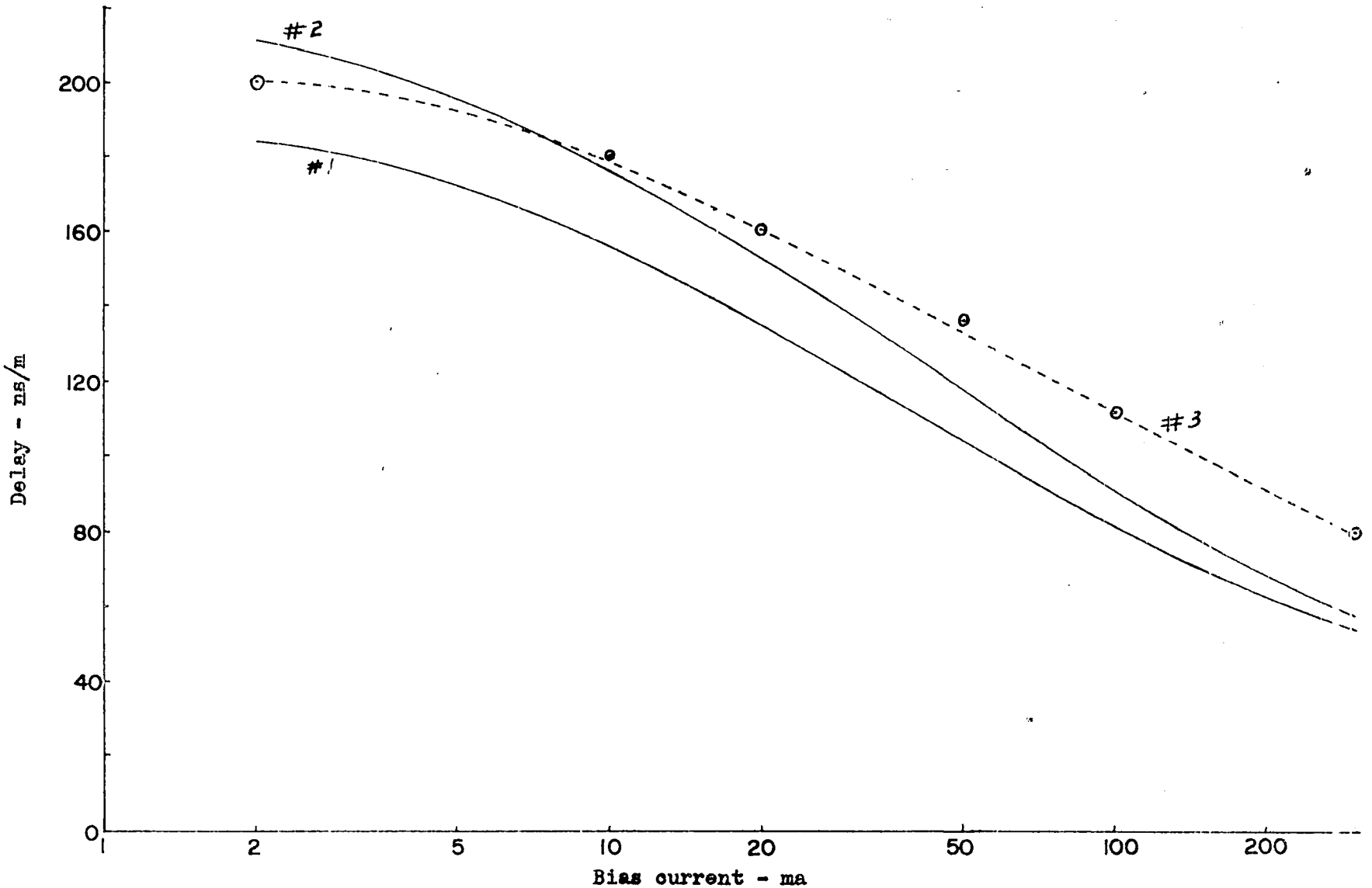

Fig. 9. Delay v. s. bias current

VI. EXPERIMENTAL RESULTS

A test line was constructed with the following parameters:

M = 10000 gauss = 1 tesla

t = 15000 A^{o} = 1.5 μ

H_k = 2.5 oe = 199 a-t/m

r_o = 2.5 mils = 63.5 μ

l = 2.5 cm = 0.025 m

R_c = 50 ohms

and the bias coil such that h_e = 100 oe/amp = 8000 a-t/m/amp. The arrangement is shown in Fig. 10. The permalloy wire was insulated from the ground plane by 2.5 mil mylar insulation. Every 2.5 cm a diode capacitor was connected from the wire to ground. The permalloy wire was direct current isolated from the input and the output by 0.003 μf capacitors. The bias voltage was brought into the permalloy wire and the capacitor diodes through a 1000 ohm resistor, this is sufficiently high to isolate the r-f. Since the inductance and the capacitance curves have similar shape the capacitor bias voltage is obtained from a resistor (R_c) placed in series with the bias coil.

A pulse was applied to the line and the output observed for different values of bias current. The results are shown in Fig. 11. The time scale is 10 ns/division and amplitude 10 mv/division. The pulses are left to right: input, outputs for bias current of 300 ma, 50 ma, 20 ma, and 2 ma. The least delayed pulse has the best shape. As the delay increases the bandwidth decreases and the pulses become more distorted. Since the pulses are different in shape the projected zero crossing is taken as the start of

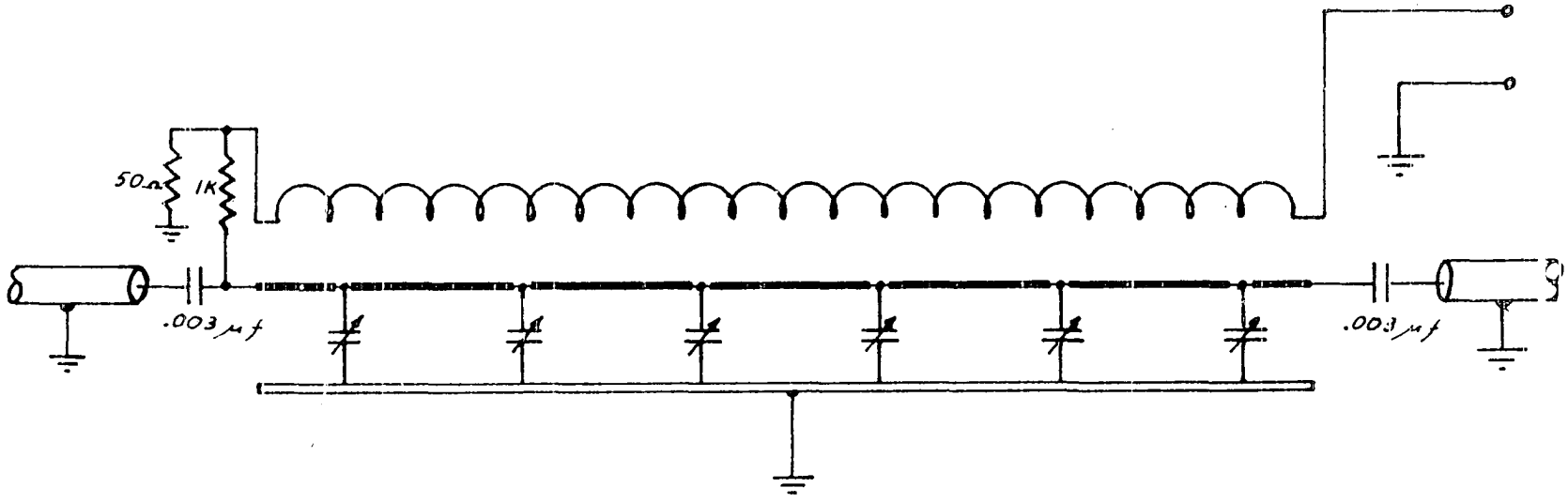

Fig. 10. Circuit of the delay line

10 mv/unit

10 ns/unit

Fig. 11. Delayed pulse

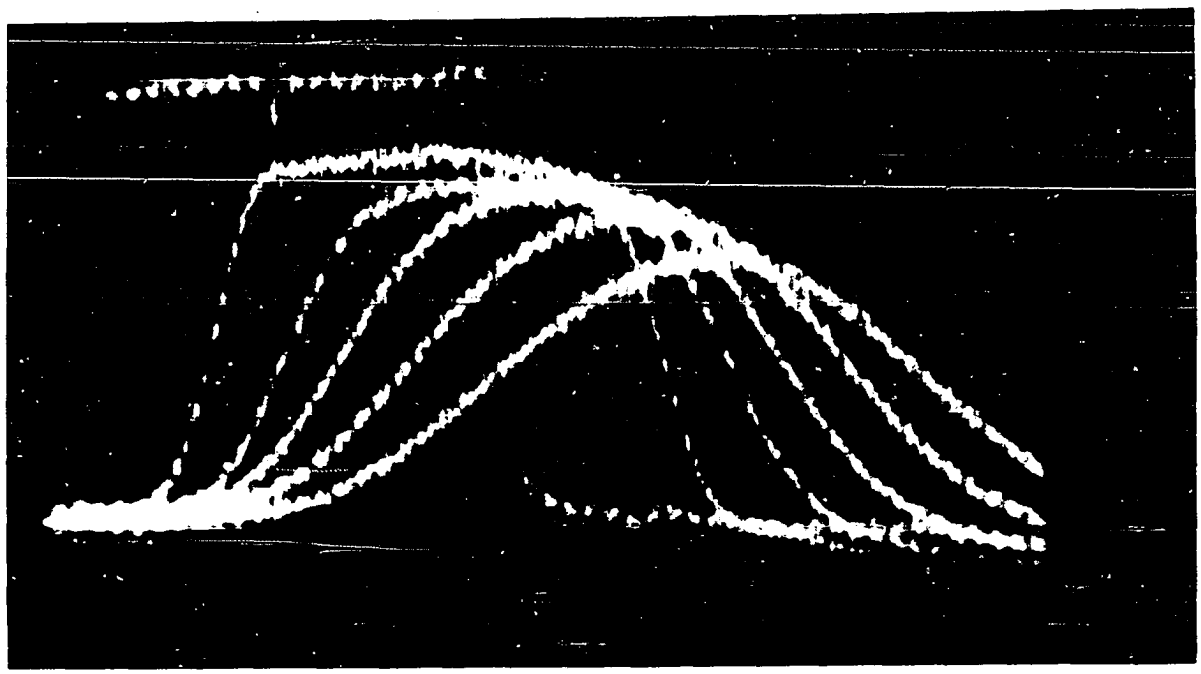

the pulse. These delays are plotted as curve #2 in Fig. 9. The experimental curve is a fairly good match to the theoretical for low values of bias. As the bias increases the depth of penetration increases and the inductance increases over that predicted by the high frequency equation. Thus the experimental curve gives larger values of delay, for high values of bias, than predicted by the high-frequency formula.

The characteristic impedance of the line was measured for various values of bias at 15 mc. The frequency was chosen to be well within the passband for high values of bias and to be near cutoff for low values. The magnitude of the experimentally determined impedance is plotted on the same graph as the theoretical impedance in Fig. 12. The theoretical impedance was calculated from the general impedance expression (equation 56). The experimental curve is parallel to the theoretical curve for low values of bias. There is a dip in the experimental curve for medium values of bias. The line has a lagging power factor for low values of bias, zero power factor at the dip, and a leading power factor for high values of bias. This would tend to indicate that the dip is caused by resonance of the end reactances of the line. This could be minimized by more careful matching at the terminations. For high values of bias the experimental curve increases rapidly. This is caused by the increase in depth of penetration beyond the thickness of the permalloy thus invalidating the inductance calculations used for the theoretical curve.

The shortness of the line has made it difficult to obtain very good data, however, the author believes that the results obtained substantiate the analytical work quite well. The line was constructed to demonstrate the feasibility rather than to give optimum performance. It was made from

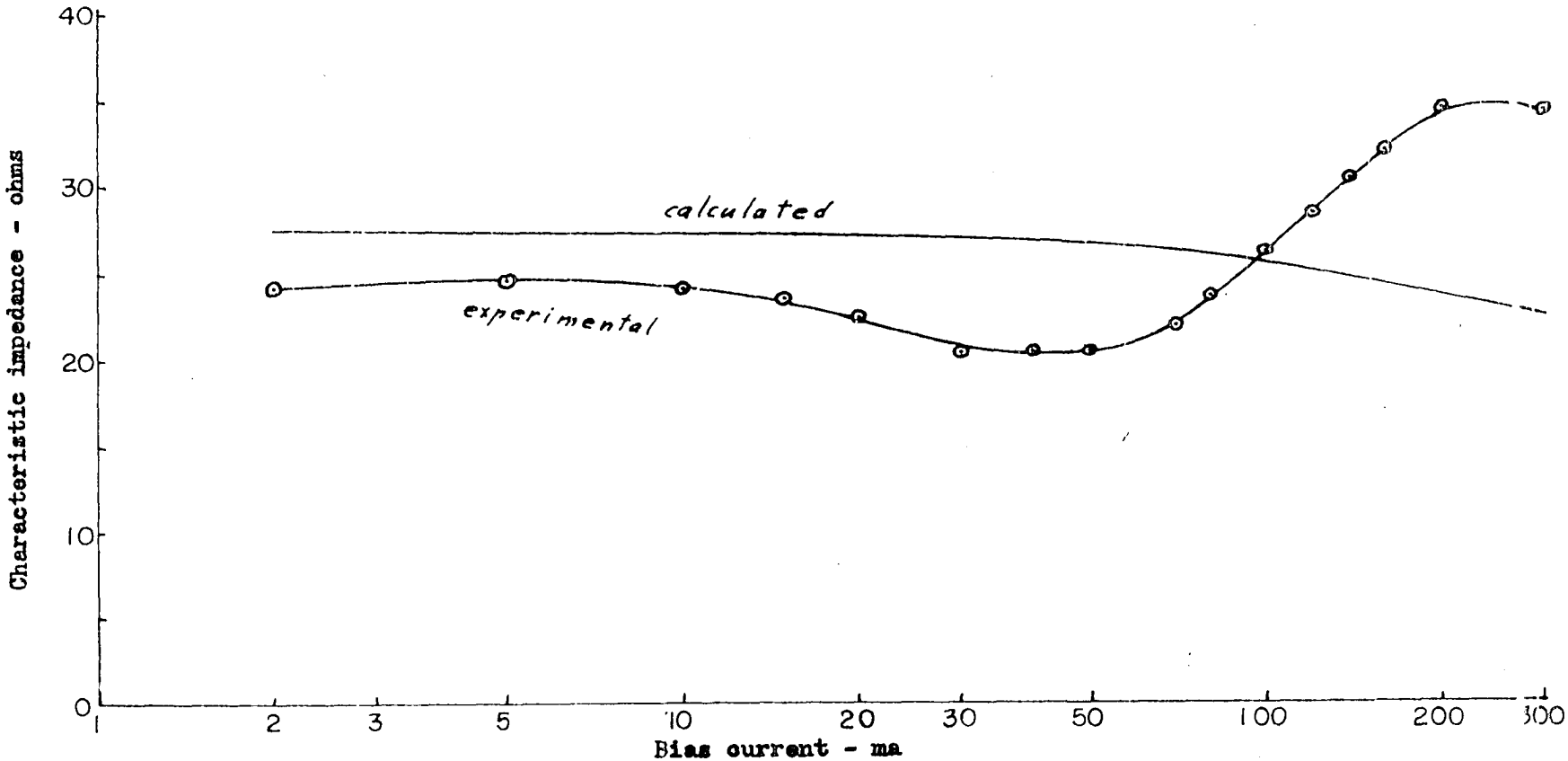

Fig. 12. Characteristic impedance v. s. applied bias

available parts and therefore separated in a poor portion of its characteristics.

VII. CONCLUSIONS

Thin film-diode capacitor variable delay lines could be built with a fairly wide bandpass and good delay characteristics. The line built here was not designed for optimum performance but more from available parts to verify the calculations. The author feels that this was accomplished within experimental error introduced by the shortness of the line. In the constructed line the velocity of propagation was about 2% that of free space. A delay change of over two to one was achieved. The thin film inevitably increases the series resistance of the line. This leads to attenuation and distortion. To minimize this resistance the film should be thin relative to the depth of penetration of the highest frequency used. This can be done by making the film physically thin or by increasing the bias to decrease the permeability and thus increase the depth of penetration. Both of these solutions to the resistance problem also tend to decrease the possible inductance change and, therefore, the change in delay. So in any given application a compromise must be reached between distortion and attenuation on one side and the range of delay on the other.

The voltage variable capacitances should be small compared to the distributed capacitance to give wide bandwidth but large for maximum change of delay. So again a compromise is necessary. For most applications a diode capacity to distributed capacity ratio of not more than 4 or 5 would give the best compromise. A better solution to the bandwidth problem would be to decrease the spacing between the variable capacitors. The ideal solution would be a distributed diode plated directly on the permalloy film. This, however, would not be easy to do.

The distortion caused by the line is caused by two sources. One is the

periodic loading of the line and the other the series resistance of the line. The distortion caused by the periodic loading, as mentioned earlier, can be reduced by a close spacing of the capacitors. In order to reduce the distortion caused by the series resistance it is possible to introduce some shunt conductance in parallel with the capacitors. If the resistance to conductance ratio is made the same as the inductance to capacitance ratio the line will be distortionless. The series resistance of the line is inversely proportional to the square root of the applied field so the shunt resistance must be proportional to the square root of the applied field. If a nonlinear resistance with the proper characteristics were found it could be placed directly in parallel with the capacitor diodes. This would not eliminate the distortion completely because the series resistance is also frequency dependent and so the best fit would be for one frequency only.

The two strongest disadvantages to this line are the cost and the attenuation. However, it is felt that its advantages: constant characteristic impedance (over a band), and the rapidly variable delay feature far outweigh the disadvantages in certain applications. The response speed is basically limited by the L-R time constant of the bias coil or the time it takes to charge up the variable capacitors whichever is larger. The capacitors can be charged in a time comparable to the delay time of the line. Since the bias coil is essentially an air coil solenoid its time constant can be controlled within wide limits set up by the bias requirements. One possible solution to the attenuation problem would be to incorporate tunnel diodes directly into the line. However, this would increase the cost somewhat.

Since no noise measurements were made it is difficult to determine con-

clusively the suitability of this line to applications in radio tele-
scopes. However, in antennas where rapid positioning is necessary and the noise not quite so critical this line presents an ideal solution. One possible use where attenuation is not of extreme importance would be in high energy physics where coincidence detection of pulses is used but the pulses do not occur at the same time. A novel used of this line would be as a matching element between a fixed impedance feed and a load with a rapidly varying impedance. Here the two ends of the wire would be connected to different voltages and the drop in the wire would bias the capacitors with progressively higher voltages. Thus the characteristic impedance of the line would gradually change and so reduce reflections.

VIII. BIBLIOGRAPHY

1. Arenberg, D. L. Basic types of delay lines. Instrumentation and Automation 31: 1679-1678. 1958.

2. Enslein, K. Remotely controlled variable delay line. Review of Scientific Instruments 28: 144. 1957.

3. Kallman, H. E. Equalized delay lines. Proceedings Institute of Radio Engineers 34: 646-657. 1946.

4. Lewis, F. D. and Frazier, R. M. Distributed-parameter variable delay lines using skewed turns for delay equalization. Proc. IRE 45: 196-204. 1957.

5. Brouneus, H. A. and Jenkins, W. H. Continuously variable glass delay line. Electronics 34: 86-87. 1961.

6. McCue, J. J. G. Semiconductor delay lines. Massachusetts Institute of Technology Lincoln Laboratory Technical Report 179. 1958.

7. Di Toro, N. J. Low dispersion wired delay lines. Institute of Radio Engineers National Convention Record 6: 82-89. 1958.

8. Dawirs, H. N. and Swarner, W. G. A very fast, voltage controlled, microwave phase shifter. Microwave Journal 5: 99-107. 1962.

9. Ince, E. L. Ordinary Differential Equations. 1st ed. New York, N. Y., Dover Publications, Inc. 1944.

IV. ACKNOWLEDGEMENTS

The author wishes to express his appreciation to his major professor Dr. R. G. Brown for his helpful suggestions during the project and during the preparation of the manuscript. The author also wishes to thank Dr. A. V. Pohm for his many suggestions during the project.